Microelectronics Reliability 168 (2025) 115660

Contents lists available at ScienceDirect

Microelectronics Reliability

journal homepage: www.elsevier.com/locate/microrel

Research paper

Thermal ageing monitoring in Cu—Al intermetallic joints through electrical resistance drift: Comparative study of lifetime potential in pure and alloyed copper wires ☆

R. Carluccio [a,*], A. Mancaleoni [a], G. Losacco [a], R. Villa [a], A. Serafini [a], L. Guarino [a], D. Dellasega [b]

[a] STMicroelectronics, Agrate Brianza, Italy
[b] Politecnico di Milano, Dipartimento di Energia, Milano, Italy

ARTICLE INFO

Keywords:
Intermetallic compounds
Reliability
Copper
Bonding process

ABSTRACT

Copper has pervasively replaced gold as preferred wire bonding material in Integrated Circuits (IC) plastic packaging. Different types of wires are available today in the market, with specific annealing treatments, coating and doping solutions aimed at optimizing bondability and reliability performances of the joints. In this study, the electrical resistance drift of packaged daisy chains has been analyzed to compare the lifetime potential of pure and alloyed copper wires under accelerated High Temperature Storage (HTS). Two aluminum-based bond-pads with different composition and thickness have been included in the experimental matrix. The results obtained through this statistically efficient and non-destructive methodology have been correlated with more "classical" readout data based on wire pull test, polished cross sections for Inter-Metallic Compounds (IMC) thickness measurement and TEM lamellas for phases stoichiometry characterization. Comparative analysis of the drift plots has pointed out a specific electrical signature for the consumption of the aluminum source under the IMC joint, confirmed by a Finite Element Method (FEM) simulation. A systematic delay in the IMC evolution has been demonstrated in all the samples with alloyed copper wires, correlating their lower ohmic drift with a lower thickness and a different composition of the IMC phases growing during HTS.

1. Introduction

Copper has progressively replaced gold in wire bonding interconnections, offering lower raw material price, higher mechanical strength, lower electrical resistance, slower intermetallic growth (when coupled with Al bond-pad) and higher thermal conductivity than Au [1]. On the other hand, copper stiffness is a permanent challenge to wire bonding in terms of process window adjustments and tailor-made choice of materials: this promoted the development and introduction of different wires features. Nowadays, there is a growing interest in alloyed copper wires, by adding elements aimed at preventing oxidation, refining grain structure, or improving reliability performances with a limited impact on package cost. Alloying elements may reduce the electrical conductivity of the wires, so further in-depth research is still necessary to identify the most appropriate solutions depending on the required product performances in all aspects [2].

The reliability of intermetallic wire bonds, like gold or copper on aluminum bond-pad, is mainly constrained by degradation mechanisms with a common influencing factor given by the geometrical, morphological, and chemical features of the IMC formed at the ball bond/bond-pad interface [3,4]. Homogeneous and evenly distributed IMCs are desirable for a good metallurgical bond forming while, during operative life, the change in their stoichiometry and the increase in thickness pose a reliability concern due to the brittle nature of specific intermetallic phases and possible tendency to voiding phenomena [5,6]. The Cu—Al IMC growth, driven by thermal diffusion of aluminum into copper, is expected to follow Eq. (1):

$$x(t)\,2 = k(T)\cdot t, \tag{1}$$

where $x(t)$ is the IMC layer thickness, t is the ageing time and $k(T)$ is the temperature-dependent diffusion coefficient given by Eq. (2):

$$k(T) = k_0 e^{-E_a/k_b T}, \tag{2}$$

☆ This article is part of a special issue entitled: 'ESREF 2024' published in Microelectronics Reliability.

* Corresponding author.
E-mail address: roberta.carluccio@st.com (R. Carluccio).

https://doi.org/10.1016/j.microrel.2025.115660
Received 19 November 2024; Received in revised form 7 January 2025; Accepted 26 February 2025
Available online 7 March 2025

where k_0 is the pre-exponential factor associated with the frequency of collisions between molecules, k_b is Boltzmann constant (8.6167×10^{-5} eV) and E_a is the activation energy, for which values in the range 0.9 to 1.2 eV can be found in literature [7,8].

As a consequence of Eq. (2), the temperature acceleration factor AF for lifetime computation (Eq. (3)) linked to temperature ageing can be effectively modeled through the well-known Arrhenius law:

$$AF_T(T_1 - T_2) = e^{[(E_a/k_b)(1/T_1 - 1/T_2)]}. \tag{3}$$

According to [2], the first intermetallic that forms during bonding is $AlCu_2$; then Cu_9Al_4 starts to appear between $AlCu_2$ and the Cu ball during ageing, and both $CuAl_2$ and Cu_9Al_4 grow simultaneously until the amount of copper increases and $CuAl_2$ transforms into Cu_9Al_4.

This work investigates the evolution of intermetallic phases during HTS in pure Cu and Cu alloy wires combined with different Al bond-pad composition and thickness. The electrical resistance variation of the Cu—Al joints has been primarily monitored, exploiting the advantages of package-level electrical readout methods: non-destructiveness, easy handling, high statistical sampling acquired in short times (the DUT consists in several joints connected in series). Guided by the resistance drift curves, ion-polished cross sections and TEM lamellas have been executed to correlate the electrical signatures with the physical changes occurring in the IMC joints. Significant differences have been observed between pure copper and alloyed copper wires, and in relation to the aluminum residual thickness under the IMC joint.

2. Experiments

Daisy chains of wire bonds have been used as test-vehicles for this study. The service chip contains peripheral rows of floating bond-pads, each one suitable to host two 60 μm-diameter ball bonds resulting after the wire bonding process from the 1.2 mils copper wires employed; the bond-pads have been obtained by laser ablation from a sputtered aluminum film over oxidized silicon substrate (see Fig. 1).

Thanks to this metal patterning technique, the test chips have been produced directly at the packaging line, thus avoiding expensive mask-making and photo-lithographic operations in the wafer fab. A plastic Thin Quad Flat Package TQFP-100L (14 × 14 × 1 mm) has been chosen to assemble the daisy chains.

The electrical testing setup has been optimized to monitor the IMC growth process through the variation of the daisy chain resistance. A resistance drift proportional to IMC growth is expected since intermetallic phases are more resistive than copper and aluminum; moreover, in the adopted ageing temperature range the absence of annealing phenomena in wires and metal bond-pads was supposed, resulting in a constant conductivity.

Given that the significant contribution to the drift derives from the growing IMC phases, gradually replacing Cu and Al, this will be a small portion of the measured resistance. Therefore, random variability and systematic errors need to be considered and prevented to achieve adequate accuracy.

The device under test is inserted in a PCB-adapter (see Fig. 2) connected to a "Keithley Model 2000" digital multimeter.

Resistance measured at each side of the package in the adopted bonding diagram is the series resistance of 44 intermetallic joints, 22 metal bond-pads and 44 wires (each one about 3 mm long). Fig. 3 reports the measurement schematic: one-shot testing approach of many joints at every readout of the HTS cells intrinsically provides a remarkable statistical depth considering the physiological variance of the individual joint resistance values and drift.

The variability coming from the wiring outside the molded component (such as multimeter cables, copper traces of the PCB adapter, spring-contacts of the socket, etc.) has been bypassed exploiting the four-pole measurement configuration schematized in Fig. 3, bringing the voltage sensing points inside the package through the first and last leads of each package side (by lead-to-lead wire bonds).

Measuring reference samples of unstressed units in parallel to the aged ones allowed to correct systematic errors between different readout sessions due to instrument offset and possibly ambient temperature: the average resistance "drift" (variation vs time-0) of the reference samples is then subtracted from each individual drift of the aged parts.

Table 1 reports the experimental cells submitted to HTS ageing in static ovens (with N_2 flux to mitigate leads oxidation), each one populated with 10 packaged daisy-chains. Bond-pads have a percentage of alloying elements ranging from 0.5 to 1 %; the main properties of the wires (purity, elongation at break and breaking load) are reported in Table 2.

Electrical resistance measurements have been performed after different ageing times for the three HTS temperatures listed in Table 3.

The equivalence between stress times at different temperatures has been estimated through Eq. 3 with an activation energy of 1.1 eV according to the most similar cases-study found in literature [6]. The first column in Table 3 shows the stress times de-rating at 150 °C, which is the typical HTS requirement for product qualification (AEC-Q100 Grade 1).

Destructive physical analysis, consisting of standard wire pull test (on a NORDSON DAGE 4000Plus bond tester), has been applied in

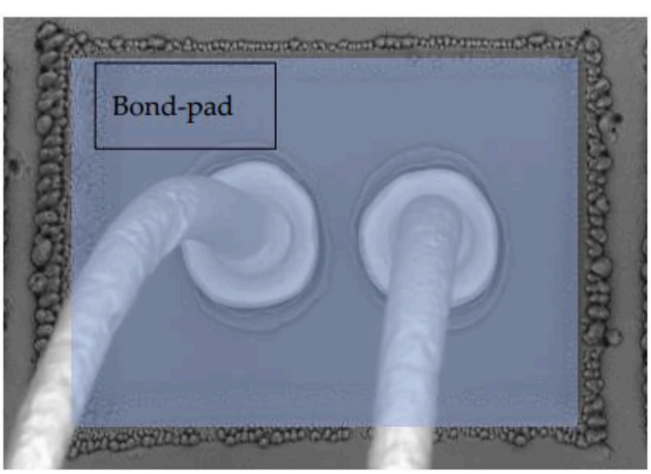

Fig. 1. Image of bond-pad with bonded wires.

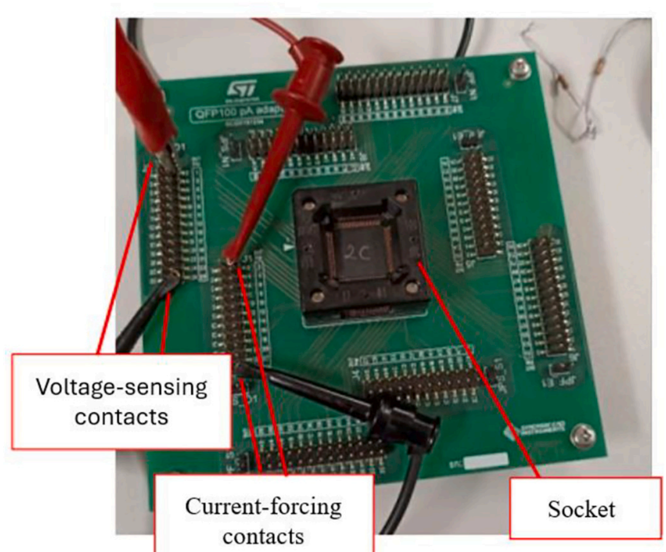

Fig. 2. Testing setup.

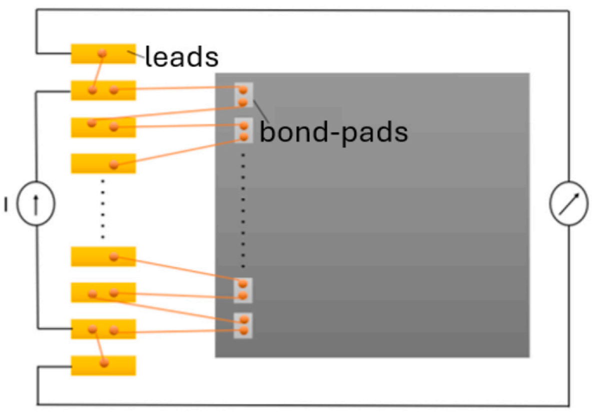

Fig. 3. Four-pole electric measurement scheme.

Table 1
List of the tested samples.

Leg	Wire	Bond-pad	Bond-pad thickness
1	Pure Cu	AlSiCu	1 μm
2	Alloyed Cu	AlSiCu	1 μm
3	Pure Cu	AlCu	3 μm
4	Alloyed Cu	AlCu	3 μm

Table 2
Wires properties.

Wire type	Purity	Elongation at break	Breaking load
Pure Cu	99.99 %	8–16 %	10–18 g
Alloyed Cu	99 %	11–21 %	16–22 g

Table 3
Electrical resistance readout matrix.

Equivalent time @150 °C (h)	$T = 175$ °C (h)	$T = 200$ °C (h)	$T = 225$ °C (h)
500	93	20	5
1000	186	41	10
1500	279	61	15
2000	372	82	20
2500	465	103	
3000	558	123	30
3500		143	
4000	743	163	40
4500		183	
5000	928	203	50
5500		223	
6000	1113	243	60

parallel to the resistance drift readout. On the most representative samples for the ageing states, identified from the resistance drift plots, investigation of IMC thickness growth rate vs time was supported by ion beam polished cross sections. Inspection at SEM also enabled the observation of IMC structure changes over time and oriented a deeper characterization by means of TEM techniques. IMC phases stoichiometry was evaluated by lamellas obtained by a Focused Ion Beam from two selected cross-sectioned bonds.

Moreover, a qualitative estimation of the current flow distribution as function of the residual aluminum thickness under the growing IMC layer has been achieved via dedicated FEM simulation. As described later in the Results section, it has been helpful to support the interpretation of the resistance drift curves obtained from the two different metal thicknesses tested in the experimental matrix of Table 3.

3. Results and discussion

Fig. 4 shows the resistance drift data obtained from 200 °C HTS. Drift data have also been collected during 175 °C and 225 °C HTS, showing the same trend in a longer and shorter stress time, respectively (example in Fig. 5).

From Fig. 4, two groups of curves are recognizable. The evidence of a higher resistance drift is related to the legs with 1 μm-thick AlSiCu bond-pads. The earlier depletion of the residual aluminum layer under the IMC has been investigated as the most probable cause for this behaviour. The hypothesis has been confirmed through a Finite Element Method (FEM) simulation on Comsol Multiphysics modeling platform. Electrical simulation has been performed considering a 2D axisymmetric geometry of wire on a pad. Electric current physics is used with a fixed electric potential as boundary condition. For the Al pad 1 μm and 3 μm thicknesses were considered, with a parametric study on IMC thickness: IMC is assumed to grow in both sides (Cu wire side for 1/3 and Al side for 2/3 of its total thickness) and the explored range is from 0 μm (no IMC case) to 2 μm. Output of these simulations is the electric current, from which the resistance variation is extracted. Finally, the IMC thickness can be associated to a HTS time, allowing a comparison with the experimental measurements. The resistivities considered were 2.4 μΩcm for the aluminum, 2 μΩcm for the copper and 14 μΩcm for the intermetallic compound (the most resistive phase was considered in the perspective of a qualitative modeling, and the value was taken from literature [2]). As reported in Fig. 6, comparing the case of IMC growth in the 1 μm-thick and 3 μm-thick bond-pad, a current crowding effect at the periphery of the ball is confirmed in the first case.

From a quantitative standpoint the simulated values in Fig. 7 are different from the experimental ones reported in Fig. 8, but the trends are comparable. Moreover, a change in the slope for the 1 μm-thick bond-pad can be noticed, corresponding to the entire aluminum depletion by the growing IMC phases.

Aluminum depletion in the 1 μm-thick bond pad was also confirmed to occur since the earliest HTS readout by the ion-polished cross sections, reported in Fig. 9. The result is a higher intermetallic compound layer thickness for the leg with available aluminum source (see Table 4).

Further evidence of the early depletion of the residual Aluminum metallization can be derived from the wire pull test, which has been performed in destructive mode. Although the pull strength values collected until the 123 h readout at 200 °C are largely above the acceptance limit applied for manufacturing control, Fig. 10 shows a partial and increasing switch of failure mode from “wire break” to “ball lift” only for the legs with 1 μm-thick metal bond-pad.

Looking at the ball lift signature in Fig. 11, the separation does not occur inside the IMC joint, that is therefore mechanically stable, but it first develops at the interface between IMC and Silicon Oxide (possibly involving the thin barrier in between), and then propagates into the oxide itself reaching the underlying silicon bulk (so-called “cratering” mode).

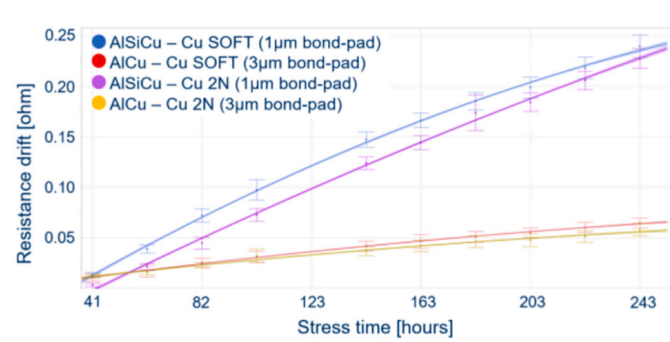

Fig. 4. Resistance drift vs 200 °C HTS time with standard deviation for the experimental points.

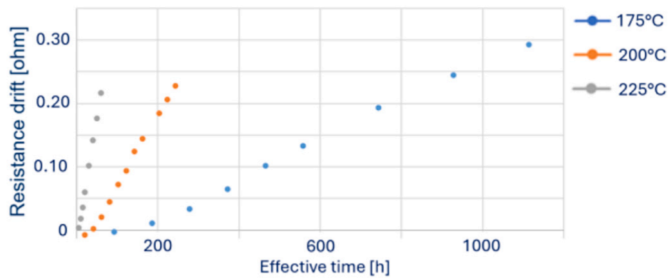

Fig. 5. Temperature dependance of resistance drift for AlSiCu – Alloyed Cu leg.

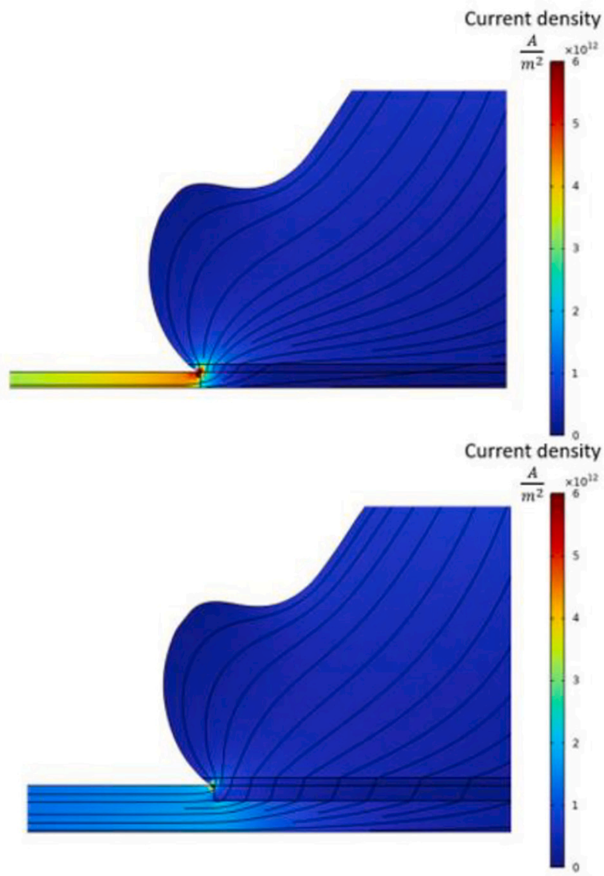

Fig. 6. Simulation of the current flux and density for a 1 μm (above) and a 3 μm-thick bond-pad (below).

Fig. 12 clarifies the bond separation path, that is quite frequent in copper bonds when the IMC layer is very close (or in contact with) the pre-metal or inter-metal dielectric: in that condition the stiffness of both Cu ball bond and related IMC joint concentrates the pull force at the bond periphery, with high probability of inducing brittle fracture in the underlying oxides in absence of the buffering effect of a significant residual thickness of aluminum metal. During a thermal ageing process this failure mode may become dominant, at least until the IMC is not affected by mechanical integrity degradation, thus becoming the weakest link.

The ball lift trends in Fig. 10 also point out that the samples bonded with alloyed Cu wires start to fail in ball lift mode significantly later than those bonded with pure Cu, confirming a certain delay in reaching the full Aluminum depletion, likely due to a slower IMC growth.

From this viewpoint, the graph in Fig. 4 also gives evidence that alloyed wires, for the same type of bond-pad metal, always resulted in a lower resistance drift versus pure copper wires.

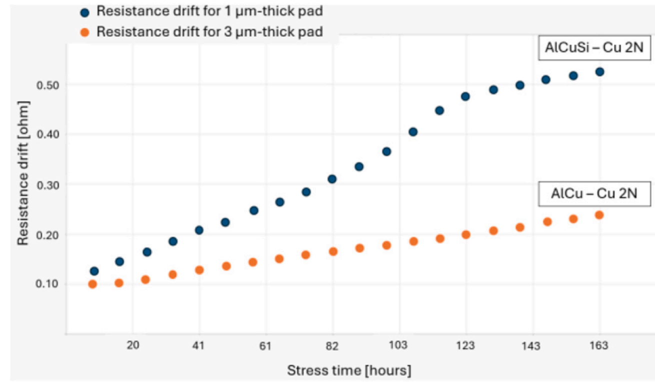

Fig. 7. Simulated values of resistance drift in time for 1 and 3 μm-thick bond-pads during 200 °C HTS.

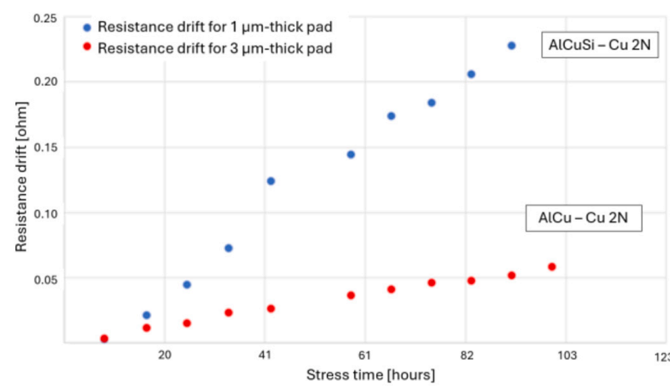

Fig. 8. Real values of resistance drift in time for 1 and 3 μm-thick bond-pads during 200 °C HTS.

Thanks to TEM analyses, stoichiometry of the intermetallic phases was extracted in two selected samples and confirmed to be in good accordance with literature [2,9]. The effect of the Alloyed Cu wire during IMCs growth was investigated considering two legs, both with 3 μm-thick bond-pads: AlCu – Pure Cu and AlCu – Alloyed Cu. They had been aged at 200 °C and analyzed after 163 h to focus on the long-term ageing effects.

Fig. 13 compares the IMCs structures of the two legs: AlCu – Pure Cu is on the left, AlCu – Alloyed Cu is reported on the right. The images are obtained by a JEOL JEM-F200 HAADF-STEM (High-Angle Annular Dark-Field Scanning Transmission Electron Microscopy). The grayscale is inversely proportional to the atomic weight of the element, so copper appears white, while aluminum is black; IMC stoichiometries are correlated with the grayscale. The residual AlCu metal (red-marked on the side of the image) is present in higher quantity in the leg with Alloyed Cu wire, where the average total thickness of the IMCs is lower. Moreover, the layering of the IMCs changes: on the right picture all the IMC layers appear to be richer in aluminum (they are darker). Also, only three different layers are present, while on the left four layers are detectable. These characteristics reinforce the hypothesis of a delaying effect of the wire alloying elements in the intermetallic diffusion, in coherence with the resistance drift measurements.

EDX (Energy-dispersive X-ray) spectroscopy was exploited to determine the stoichiometry of the phases present in both legs.

The results obtained from AlCu – Pure Cu are reported in Fig. 14. Looking at aluminum and copper elemental maps, the four layers are clearly visible. As expected, the amount of aluminum is higher the closer to the pad, and decreases moving towards the wire. Copper content follows the opposite trend. The wire is 99.99 % copper, hence no other

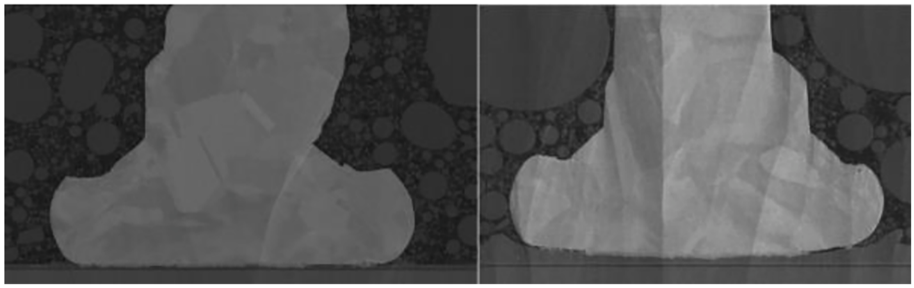

Fig. 9. Ion polished cross section of 1 μm AlCuSi – Pure Cu (on the left) and 1 μm AlCu – Alloyed Cu (on the right) after 82 h ageing at 200 °C.

Table 4
IMC layer thickness during 200 °C HTS.

Leg	Thickness at 82 h (μm)	Thickness at 163 h (μm)
1 μm AlSiCu – Pure Cu	0.69	0.87
1 μm AlSiCu – Alloyed Cu	0.59	0.7
3 μm AlCu – Pure Cu	0.74	1.12
3 μm AlCu – Alloyed Cu	0.65	0.82

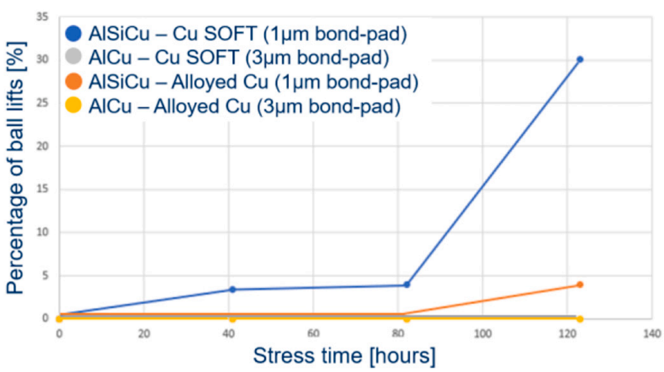

Fig. 10. Ball lift occurrence trend at wire pull test vs time for samples aged at 200 °C.

Fig. 11. Ball lift signature of legs with 1 μm-thick bond-pad after being subjected to 200 °C HTS.

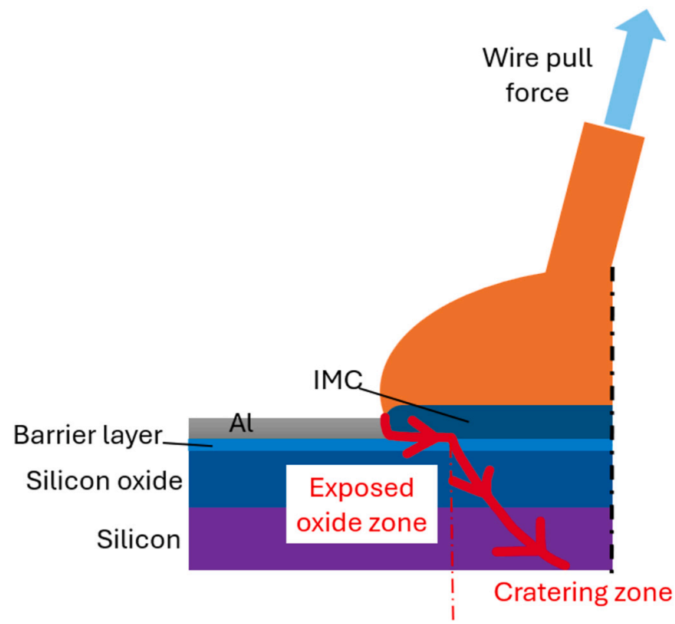

Fig. 12. Bond separation path after wire pull when IMC layer is close or in contact with the pre-metal dielectric.

element was detected by the chemical analysis.

A comparison with [2] made it possible to assign the corresponding stoichiometry to each detected phase. Results are shown in Fig. 15. The percentages of copper (in blue) and of aluminum (in green) are reported. The percentage of aluminum in Intermetallic 1 is so low that it is considered pure copper in [2]. The most stable phase after ageing, Cu_9Al_4, has formed. Intermetals 3 and 4 have different amounts of copper and aluminum but are analogous according to [2]. The intermetallic compound phase richer in aluminum, $CuAl_2$, is not present anymore. Most probably, it has already converted in CuAl.

For the AlCu – Alloyed Cu sample, EDX is reported in Fig. 16. From aluminum and copper boxes the presence of three layers can be noticed. As previously highlighted, the residual aluminum has a higher thickness with respect to the AlCu – Pure Cu leg. Our hypothesis considers the arrangement of alloying atoms at the grain boundaries as the cause of the observed delay in the IMCs growth, by hindering the Al diffusion. However, EDX was not sufficient to confirm this theory due to its intrinsic detection threshold (alloying element clustering at the grain boundaries does not appear from the map). The correct stoichiometry is associated to each layer in Fig. 17.

Intermetallic 1 is considered pure copper because of the low percentage of aluminum. The phase richer in aluminum is not present here. The only intermetallic phase detected is CuAl. From the comparison with the AlCu – Pure Cu results, we can say that the main difference is the absence of Cu_9Al_4 in the AlCu – Alloyed Cu. Probably, Cu_9Al_4 is the dominant phase that is here not formed yet because of the delay induced by the impurities in the wire. Cu_9Al_4 might be found in AlCu – Alloyed Cu legs for longer times than those reached in this study.

The polished cross sections performed at the different stress temperatures have also been exploited to collect sample data-points for IMC thickness. With the limitation of a low statistical sampling, the hypothesis initially made for the growth model and the acceleration factors

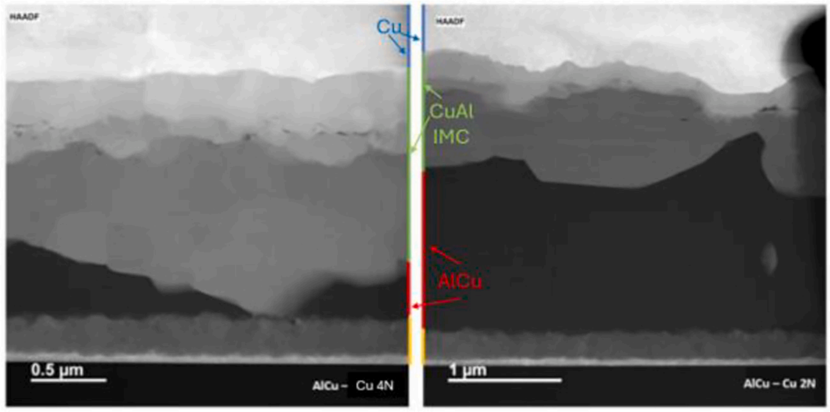

Fig. 13. Comparison by STEM acquisitions of AlCu - Pure Cu on the left and AlCu - Alloyed Cu on the right after 200 °C ageing for 163 h.

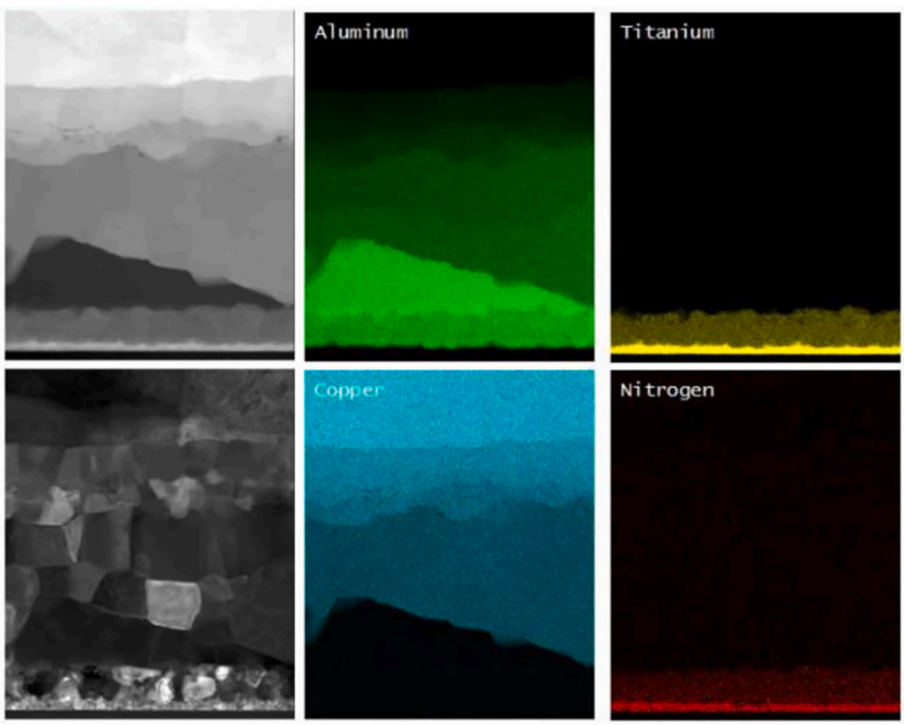

Fig. 14. STEM-HAADF/DF micrographs and respective EDX elemental maps of AlCu–Pure Cu leg aged at 200 °C for 163 h.

has been checked by comparing the average thickness values at the equivalent durations computed with Ea = 1.1 eV and previously presented in Table 3. Fig. 18 shows the fitting of the data points at 200 °C by Eq. (1) for the experimental leg combining AlCu 3 μm-thick metal with Pure Cu wire, de-rated at 150 °C as common reference time scale. The red dot in the graph corresponds to the average IMC thickness measured after the equivalent HTS duration at 175 °C estimated with the above activation energy. The assumption looks therefore reasonable, as the data-point at 175 °C overlaps the variance range calculated for the corresponding point of the 200 °C growth curve. The time dependance law adopted through Eq. (1) (also normally used for diffusion-limited oxidation of silicon in "Deal-Grove" model) may be object of deeper assessment by increasing the frequency and sampling size of IMC thickness measurements. In this perspective the value of the activation energy will be estimated with higher confidence level, too.

4. Conclusions

This work was useful to understand the influence of copper wire type and bond-pad metal thickness on the evolution of AlCu intermetallic joints under high temperature ageing, tightly correlated with the achievable lifetime for the Integrated Circuits adopting copper wire-bonding interconnections.

The monitoring of electrical resistance drift has been demonstrated to be a powerful and highly efficient method to characterize the behaviour of different wire/bond-pad combinations.

A significant delay in the CuAl IMC joints interdiffusion mechanisms can be obtained when using Alloyed Cu wires instead of Pure Cu wires: even if no wearout has been observed in the solder joints after remarkable ageing times, a higher lifetime potential is expected from doped Cu wires, which can therefore be considered as good candidate in front of ICs usage profiles characterized by constantly high operating temperature and/or extended service time in the field (e.g. Automotive).

The wearout of intermetallic compounds has not been reached yet,

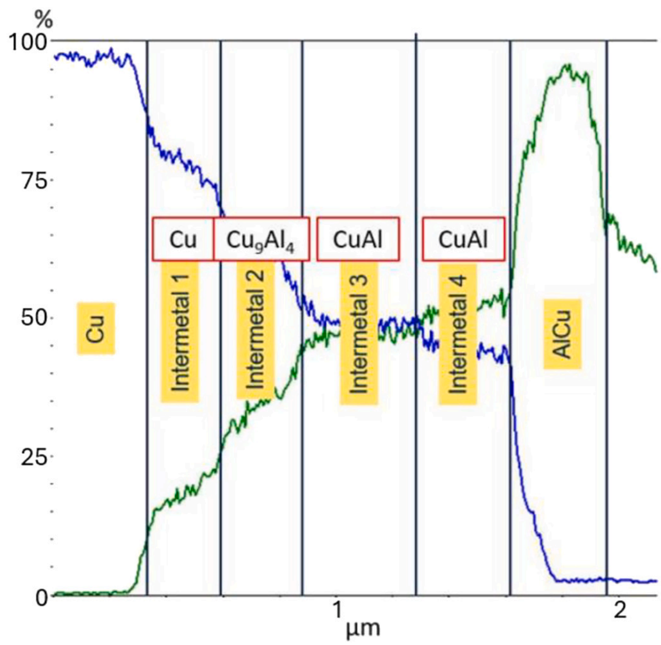

Fig. 15. Copper and Aluminum % profile of the IMCs after 163 h HTS 200 °C for AlCu – Pure Cu leg.

and this opens the opportunity for further investigation of the phenomena after longer ageing. Additional data about IMC thickness would also enable a fine-tuning of the activation energy value and the IMC growth law given by Eq. (1).

CRediT authorship contribution statement

R. Carluccio: Validation, Formal analysis, Investigation, Resources, Data curation, Writing – original draft, Visualization. **A. Mancaleoni:** Conceptualization, Methodology, Investigation, Writing – review & editing, Supervision, Project administration. **G. Losacco:** Investigation, Writing – review & editing. **R. Villa:** Conceptualization, Methodology, Resources, Writing – review & editing, Supervision, Project administration, Funding acquisition. **A. Serafini:** Investigation, Resources. **L. Guarino:** Software, Investigation. **D. Dellasega:** Writing – review & editing, Supervision, Project administration.

Declaration of competing interest

The authors declare the following financial interests/personal relationships which may be considered as potential competing interests: Roberta Carluccio reports administrative support was provided by

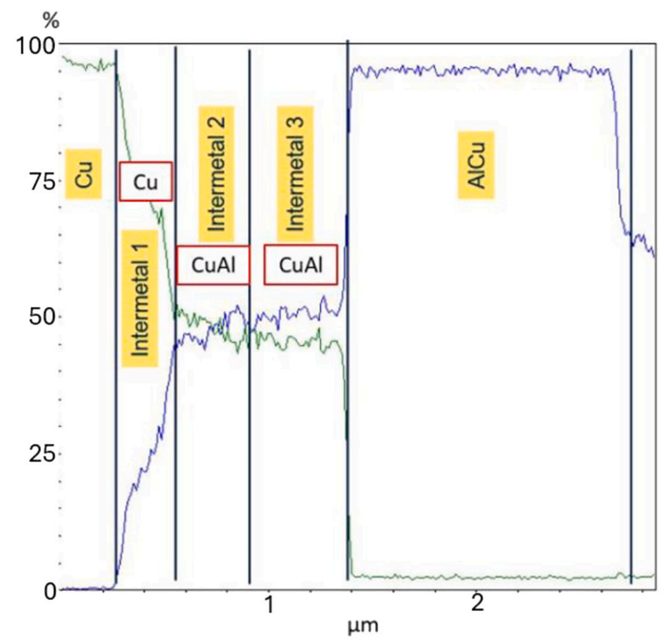

Fig. 17. Copper and Aluminum % profile of the IMCs after 163 h HTS 200 °C for AlCu – Alloyed Cu leg.

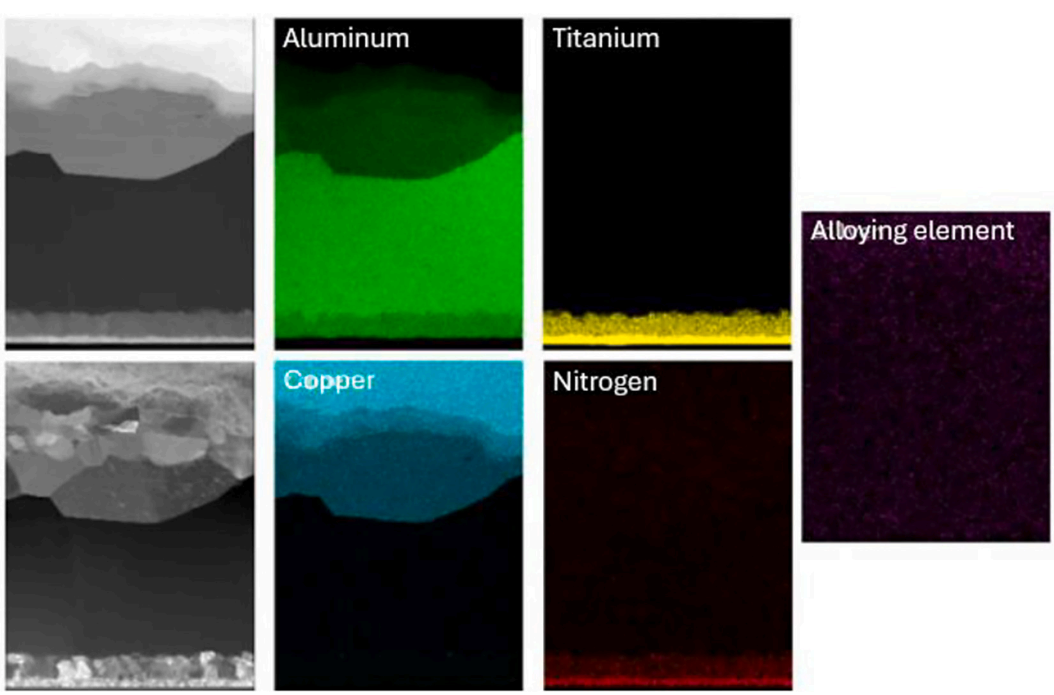

Fig. 16. STEM-HAADF/DF micrographs and respective EDX elemental maps of AlCu – Alloyed Cu leg aged at 200 °C for 163 h.

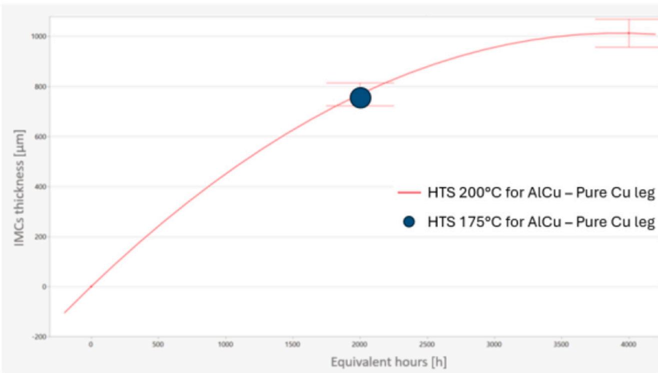

Fig. 18. Square-root fit of IMC thickness vs equivalent time at 150 °C for AlCu – Pure Cu leg after HTS 200 °C, and the overlapping experimental point at 2000 h HTS 175 °C.

Polytechnic University of Milan - Milano Leonardo Campus. If there are other authors, they declare that they have no known competing financial interests or personal relationships that could have appeared to influence the work reported in this paper.

Data availability

No data was used for the research described in the article.

References

[1] Alberto Mancaleoni, et al., Copper wire bonding process characterization and simulation, in: CIPS 2020; 11th International Conference on Integrated Power Electronics Systems, VDE, 2020.

[2] Preeti Chauhan, Z.W. Zhong, Michael Pecht, Copper Wire Bonding, Springer, New York, 2014.

[3] G. Harman, Wire Bonding in Microelectronics, third edition, McGrawHill, 2010.

[4] G.E. Servais, S.D. Brandenburg, Wire bonding-a closer look, in: The 17th International Symposium for Testing & Failure Analysis, 1991.

[5] R. Enrici Vaion, et al., Thin copper wire under extreme HTSL stress duration: crack failure mechanism characterization, in: 2016 IEEE 18th Electronics Packaging Technology Conference (EPTC), IEEE, 2016.

[6] Z.W. Zhong, Wire bonding using copper wire, Microelectron. Int. 26 (1) (2009) 10–16.

[7] Hyoung-Joon Kim, et al., Effects of Cu/Al intermetallic compound (IMC) on copper wire and aluminum pad bondability, IEEE Trans. Comp. Packag. Technol. 26 (2) (2003) 367–374.

[8] Chwee Sim Goh, et al., Corrosion study and intermetallics formation in gold and copper wire bonding in microelectronics packaging, Crystals 3 (3) (2013) 391–404.

[9] C.J. Hang, C.Q. Wang, M. Mayer, Y.H. Tian, Y. Zhou, H.H. Wang, Growth behavior of Cu/Al intermetallic compounds and cracks in copper ball bonds during isothermal aging, Microelectron. Reliab. 48 (3) (2008) 416–424.